A Numerical Investigation of Stress Distribution in Ship Deck Stiffener Panel Structures under Uniformly Distributed Load

Tengyang Fu[1], Leyang Xie[2] and Zhehao Xu[3, *]

[1]School of Civil Engineering, Central South University, Changsha, Hunan, 410000, China

[2]School of Geosciences and Info-physics, Central South University, Changsha, Hunan, 410000, China

[3]Department of Civil Engineering, University of British Columbia, Vancouver, British Columbia, V6T 1Z4, Canada

* Corresponding Author Email: xzh27@student.ubc.ca

Abstract. Ship decks are commonly composed of stiffener panel structures, which consist of flat plates, longitudinal stiffeners, and transverse girders. These steel stiffener panels are subjected to significant loads when carrying cargo. This study aims to simulate the behaviour of stiffener panel structures under uniformly distributed load and identify the value of extreme stresses experienced by the structure and their corresponding locations. The results obtained provide valuable insights for optimizing and reinforcing the design of stiffener panel structures in the future. The research is divided into two main parts. Firstly, a finite element model of the stiffener panel structure was developed to obtain numerical simulation. Traditional holistic modelling of large deck structures can be time-consuming; hence, this part of the study focuses on proposing a simplified modelling approach while ensuring acceptable level of accuracy. The second part of the study involves utilizing existing theories, including Euler-Bernoulli beam theory and plate bending stress formulas introduced by Timoshenko and Roark, to calculate theoretical stress values at the critical locations determined in the first part. The calculated stress results were compared with the finite element analysis from the first part to validate the accuracy of the established model. The final results demonstrate excellent agreement between the outcomes obtained in the first and second parts of the study, confirming the validity and reliability of the approach used for stress analysis in stiffener plate structure.

Keyword: Critical normal stress, von Mises stress, finite element analysis, stiffened panels, plate bending.

1. Introduction

Stiffener panel structures play a significant role in diverse domains such as maritime, aerospace, and bridge engineering. In the maritime sector the primary weight-bearing framework of the vessel's hull often comprises interconnected cross-stiffened panels. These cross-stiffened panels typically consist of plates, longitudinal stiffeners, and transverse girders. Operating in marine environments, vessels must withstand a complex array of loads, including wave-induced forces, wind pressures, and cargo weights. The inclusion of stiffeners enhances structural integrity by distributing external forces, thereby ensuring stability and preservation of the vessel's structural integrity.

Numerous studies have explored the mechanical properties of stiffened panel structures. Noteworthy among these investigations is the work of Zhang et al. [1], who identified six distinct failure modes of stiffened panels under uniaxial compression. Zhang et al. [1] conducted numerical analyses to propose evaluation formulas for each failure mode. Furthermore, Xu and Soares [2] experimentally determined the ultimate strength of stiffened panels subjected to uniaxial compression. Most investigations to date have predominantly focused on the response of stiffened panels under axial compression, primarily due to the susceptibility of thin-wall stiffened panel structures to buckling. Consequently, buckling failure modes tend to govern the design process for most loading scenarios. However, the various geometric configurations and loading conditions of stiffened panels result in a multitude of potential failure modes. For instance, in cases where local stress exceeds yield

stress, plastic deformation occurs, leading to permanent structural damage or failure. This underscores the importance of avoiding such failure modes in practical applications.

This susceptibility to failure is particularly relevant in ship deck applications. Ship decks frequently bear substantial cargo loads, imposing tensile and compressive stresses on underlying stiffeners and girders due to internal moments. Platypodis [3] employed finite element modeling to assess stress distribution in cross-stiffened panels subjected to uniformly distributed loads. However, his research did not extensively elaborate on the specific values and locations of extreme stresses within the model. In a similar vein, Kim et al. [4] proposed an optimized method for setting the boundary conditions for stiffened panel in finite element modeling.

Expanding on existing research, this study seeks to numerically simulate the precise values and locations of internal extreme normal forces, shear forces, and von Mises stresses within stiffened panels under uniformly distributed loads. Platypodis [3] found that the local bending stress distribution in cross-stiffened panels can be decomposed into stress components from beam bending ($\sigma 1$) and plate bending ($\sigma 2$). The actual stress state can then be computed as the sum of $\sigma 1$ and $\sigma 2$, following separate calculations of their respective values.

Various scholars have previously proposed approaches for computing bending moments and bending stresses in plates under different boundary and loading conditions. Notable formulations include those presented by Timoshenko [5], Young [6], and Wojtaszak [7]. Osadebe and Aginam's research synthesized these methods and established a more precise calculation technique based on the Ritz variational approach. Subsequently, the maximum bending stress in the plate can be computed using classical plate theory, with formulas elucidated by Kelly. Meanwhile, the bending stress resulting from beam bending ($\sigma 1$) can be determined using classical Bernoulli-Euler beam theory [8, 9].

This analysis will be facilitated by developing a Finite Element Model of the stiffened panel using Femap software. The outcomes of the Finite Element Analysis (FEA) will be rigorously compared with results derived from established theories and prior research findings. This comparative approach serves to authenticate and establish the accuracy and dependability of the FEA technique. Through these efforts, a deeper comprehension of cross-stiffened panel behavior and structural responses is anticipated, contributing to the refinement of design and analysis methodologies for such structures.

2. Establishment of the Finite Element Model

Stiffened panel structures often exhibit significant dimensions, posing challenges when attempting to analyze the entire structure using Finite Element Method. The computational capacity of FEA software typically restricts the number of element nodes that can be defined due to computer memory limitations. To create a model with a constrained number of element nodes, the mesh size defining the model must be increased. However, employing larger element sizes in FEA software can be problematic as the outcome of the analysis are derived through numerical approximations. Such a practice can result in inaccuracies, frequently causing an underestimation of stress within the structure. Furthermore, performing analyses on substantial and complex finite element models consumes a significant amount of time, rendering it practically unviable.

Fricke et al. [10] proposed an approach to simplify finite element modelling (FEM) of stiffened panels. This approach centered on the concept of modeling a specific section of the structure, while also applying appropriate boundary conditions to replicate the supportive effects exerted by interconnected components. Through various investigations, Fricke et al. explored strategies for simplifying the model and discovered that the two-span (½-1-½ model) stiffened panel model produced satisfactorily accurate results [10]. Building upon their insights, the current study adopts a similar approach, focusing on a specific section illustrated in figure 1. The full width of the stiffened panel was modeled as no boundary conditions could emulate the deflected shape along the girders once loaded. The stiffened panel is divided in the direction of the stiffeners. Consequently, only half

of the stiffener span on both sides is integrated into the model. The modeled section is shown in figure 2 [11].

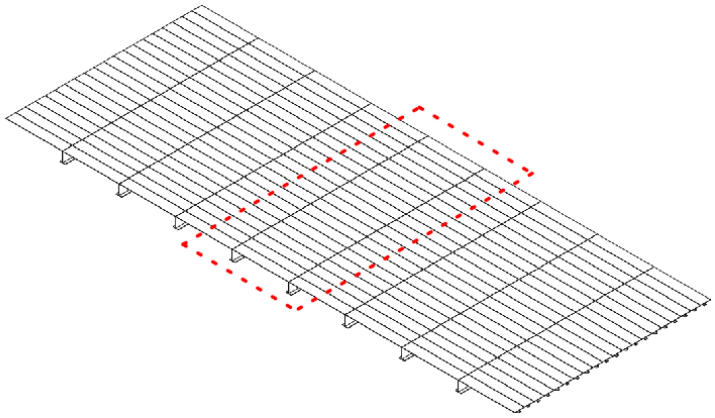

Figure 1. The modeled section of the entire stiffened panel.

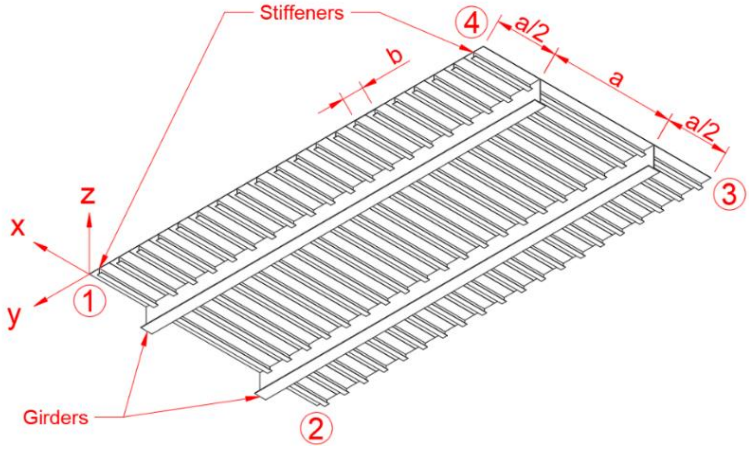

Figure 2. Schematic view of the modeled stiffened panel.

The specified boundary conditions for the model are presented in table 1. To emulate the behaviour of the stiffened panel when utilized as a ship deck, fixed boundary conditions have been imposed on the ends of the girders. This is informed by the anticipation that the stiffened panel, in its role as a ship deck component, will be affixed along all its edges. This connection is expected to have strong rigidity, effectively preventing rotational and displacements in all directions.

Table 1. Boundary condition of the finite elemnt model [a].

Panel edges	Boundary Condition
1-2 and 3-4	Fixed support condition with Rx = Ry = Rz = 0 Tx = Ty = Tz = 0
1-4 and 2-3	Ry = 0 Tx = 0 (Additional constraint)

[a] Stiffened Panel Model Found in Figure 1

Constraints are placed on the termini of the stiffeners with specific regard to rotational movement around the x-axis. This constraint is rooted in the assumption that the resulting deflected shape of the stiffener will closely mimic the pattern illustrated in figure 3. This prescribed boundary condition serves to maintain the continuity of the deflected shape at the stiffener ends. The details of the dimensions of the modelled stiffener panel and the cross-section of the stiffener and girder are summarized in table 2. All corresponding parameters are defined in figure 4.

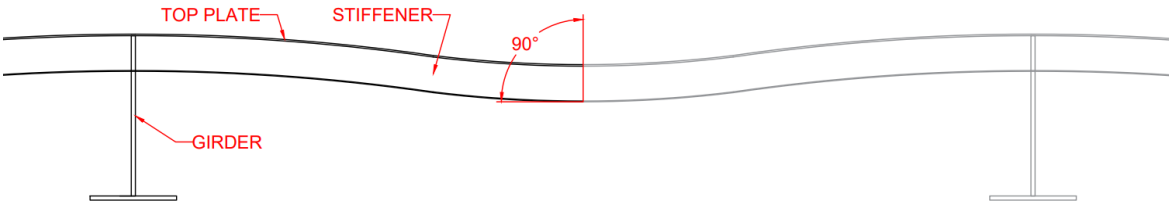

Figure 3. Anticipated deflected shape of the top plate and stiffener.

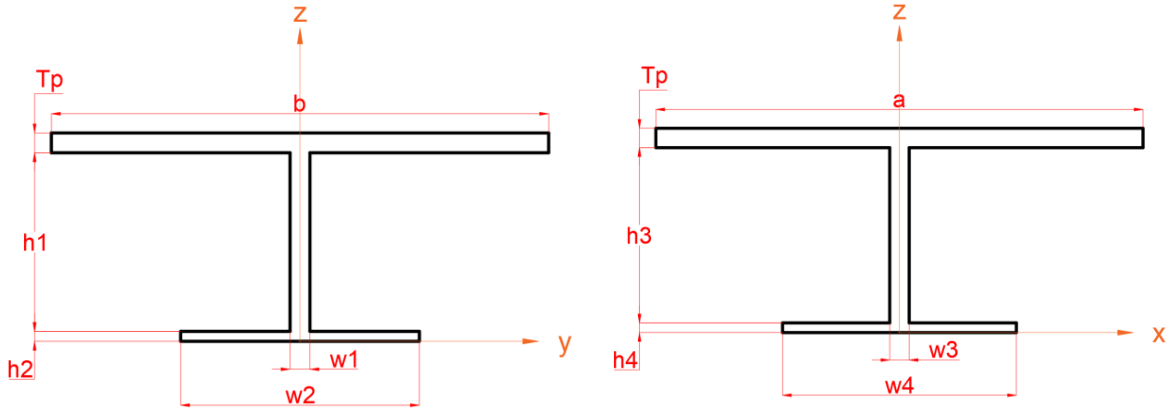

(a) (b)

Figure 4. Cross-section of the structure elements (a) Cross-section of the stiffener; (b) Cross-section of the girder (Note: drawing not to scale).

Table 2. Geometric parameter of stiffened panel.

Description	Variable	Length (mm)
Stiffener spacing	b	900
Girder spacing	a	5,200
Thickness of top plate	Tp	9
Height of stiffener's web	h1	200
Width of stiffener's web	w1	4
Height of stiffener's flange	h2	4.5
Width of stiffener's flange	w2	200
Height of girder's web	h3	920
Width of girder's web	h4	24
Height of girder's flange	w3	24
Width of girder's flange	w4	500

The selected section's numerical analysis is conducted utilizing the FEM software Femap. For modeling the stiffened panel structure, which primarily comprises thin plates, the shell element approach is employed. This choice is motivated by its potential to yield accurate results while also minimizing the overall model size. The meshing strategy involves utilizing a mesh size of 50mm x 50mm for all surfaces spanning the x-y plane, and a mesh size of 50mm x 20mm for surfaces spanning the z-y plane. This meshing approach aims to ensure proper alignment of element nodes and to maintain a consistent mesh size across the majority of the model components.

A uniform pressure (p) of 20 kPa is applied to the plate in the model. The structural material assigned to the model is standard steel, characterized by a Young's modulus of elasticity (E) equal to 210 GPa and a Poisson's ratio (υ) of 0.3. Since this study primarily aims to analyze the stress distribution resulting from the applied load, the gravitational self-weight of the material is disregarded [6].

Upon analyzing the Femap model, it was observed that at the ends of the stiffener, there was a deflection pattern characterized by the rotation of its edge in the y-axis direction as shown in figure 5. This observation contradicted the initially defined constraint and resulted in inaccurate outcomes.

Notably, stress values derived from the stiffener's edge greatly diverged from those obtained at the mid-span of the stiffener situated between the girders. This discrepancy indicated a failure in accurately emulating the authentic support conditions experienced by the stiffener.

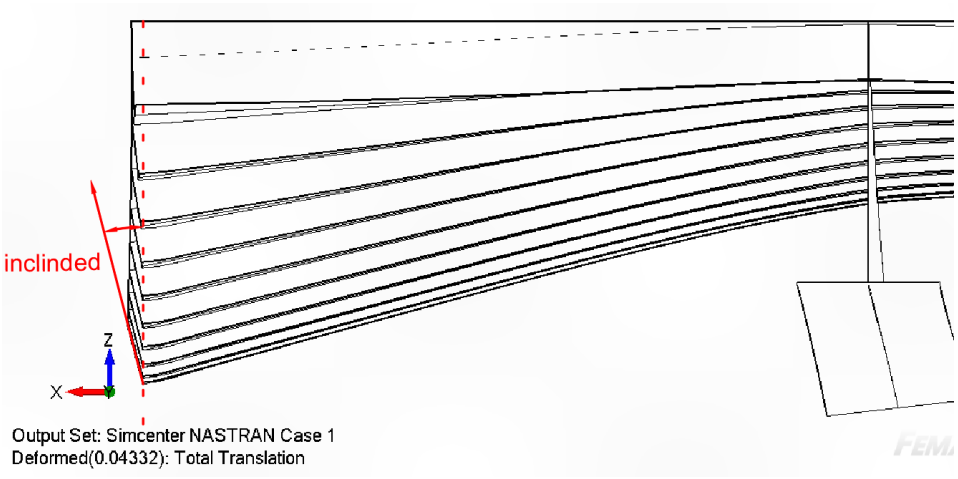

Figure 5. Rotation at the edges of the model.

Consequently, it was established that the existing constraints were inadequate. To address this issue, an additional constraint was introduced for the stiffener's edges. This constraint restricts the displacement of the stiffener in the x-axis direction. This constraint was formulated based on the presumption that the spacing between the girders and the overall length of the stiffener panel remain unchanged under the applied load. This assumption stems from the anticipation that the stiffener panel is rigidly supported at all its edges.

3. Result of FEM Analysis

3.1. Analysis of normal stresses

The deflected configuration of the model is visualized in figure 6. Upon scrutinizing the model, it was discerned that the stiffener connected to the midpoint of the girders endured the most significant normal stress, rendering it representative. Investigation into the stress distribution on this stiffener revealed that normal stress concentrated at three specific locations, as delineated in figure 7. These locations are further depicted in figure 8 in the cross-sectional view of the stiffener. The corresponding stress values for these locations are presented in table 3, indicating the maximum and minimum values.

While the stiffener is primarily subjected to normal stress in the x-axis direction, the girders predominantly endure stress along the y-axis direction. Notably, the ends of the girder manifest the highest positive and negative normal stresses. These extremities of the girder correspond to the positions delineated in figure 9. These locations are further depicted in figure 10 in the cross-sectional view of the girder and the exact stress values are outlined in table 3.

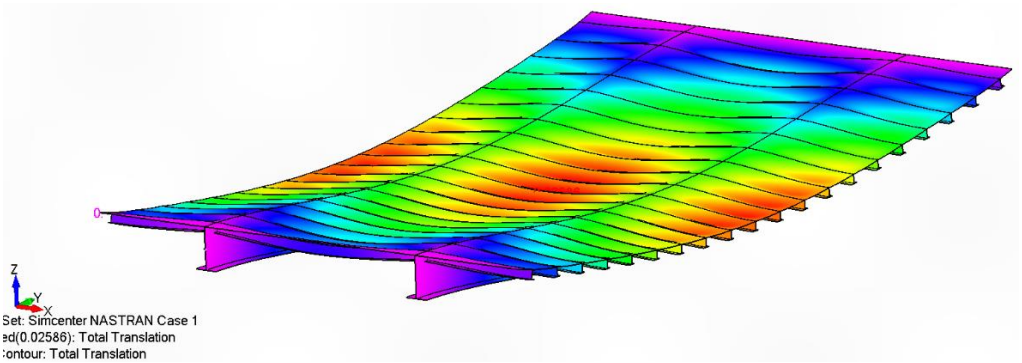

Figure 6. Deflected shape of the stiffened panel.

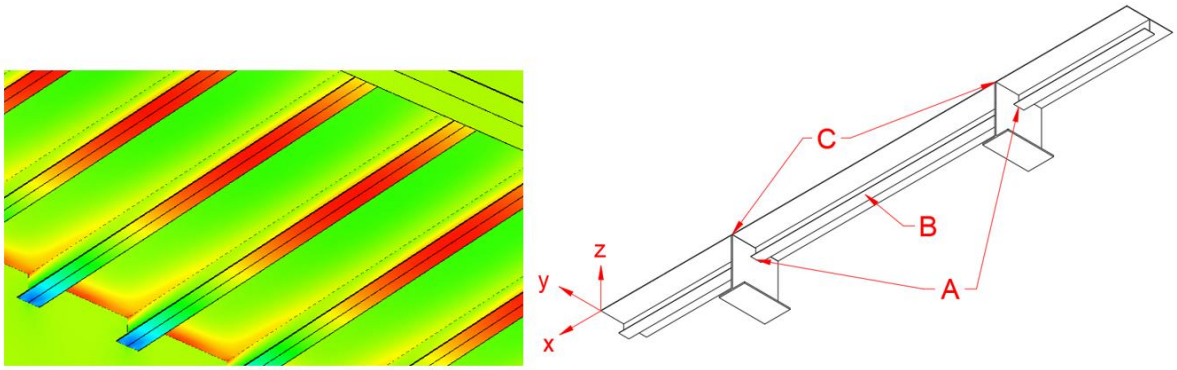

Figure 7. Labeled points of interest for normal stress values on the stiffener.

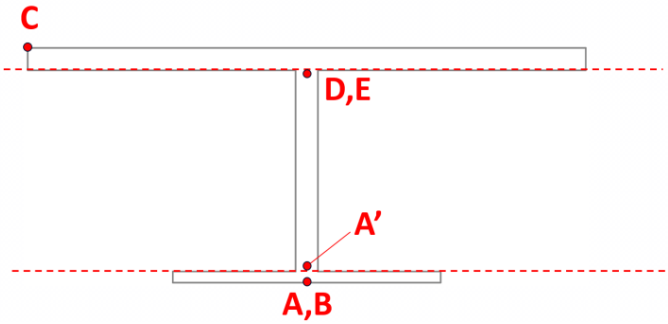

Figure 8. Labeled points of interest on the cross-sectional view of the stiffener.

Table 3. Value of the stresses at the points of interest from FEA.

Points	Location	Stress Type	Stress Direction	Stress Value (Mpa)
A	The stiffener connected to the mid-span of the girders	Normal Stress	X	-184.79
B				94.30
C				88.02
G	Girder		Y	200.47
H				-246.1
		von Mises Stress	/	225.78
D	The second stiffeners from the plate boundary	Shear Stress	XY	60.73
E				-60.73
A'	The stiffener connected to the mid-span of the girders	von Mises Stress	/	186.58
G'	Girder			188.66

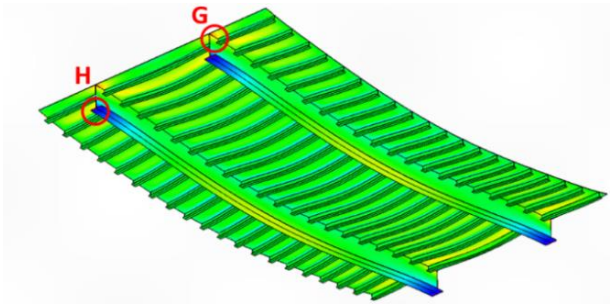

Figure 9. Labelled points of interest on the girder.

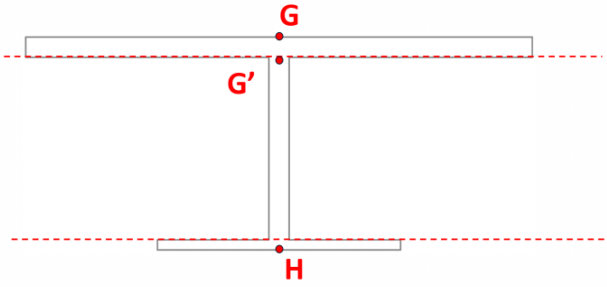

Figure 10. Labelled points of interest on the cross-sectional view of the girder

3.2. Analysis of shear stresses

The color-contour representation of shear stress from the Femap analysis reveals that the most significant shear stresses, both maximum and minimum, are situated at the upper tip of the second stiffener (from the boundary of the plate) on opposite ends, as depicted in figure 11. In this figure, the plate is omitted to enhance the clarity of stress distribution at the stiffeners. The specific locations are outlined in detail in figure 8 within the cross-sectional view of the stiffener, and these are denoted as points D and E. Point D corresponds to the location of maximum shear stress, while point E represents the location of minimum shear stress. Detailed stress values are concisely presented in table 3.

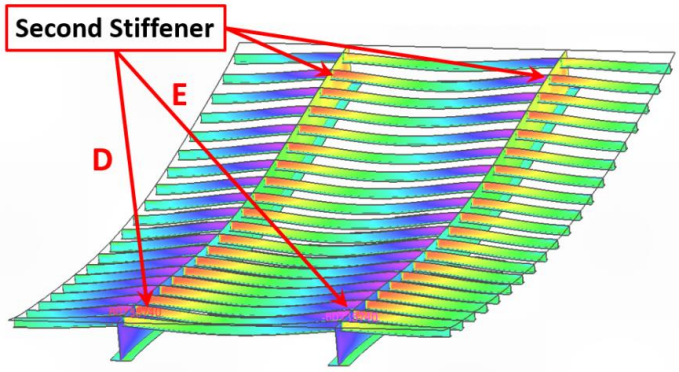

Figure 11. Demonstration of the stiffeners exposed to maximum and minimum shear stresses.

3.3. Analysis of von mises stresses

The von mises stresses exhibit notable concentration at specific locations within the stiffened panel, as visually depicted in figure 12. Please note that in this illustration, point A serves for illustrative purposes only. It demonstrates that von Mises stresses reach a local maximum at the bottom of the stiffener where it is connected to the girder. However, this depiction does not indicate that the stiffener showcased in the figure harbors the maximum von Mises stresses. In fact, the central stiffener, affixed to the midpoint of the girder within the panel, stands as representative and bears the highest von Mises stresses among all the stiffeners.

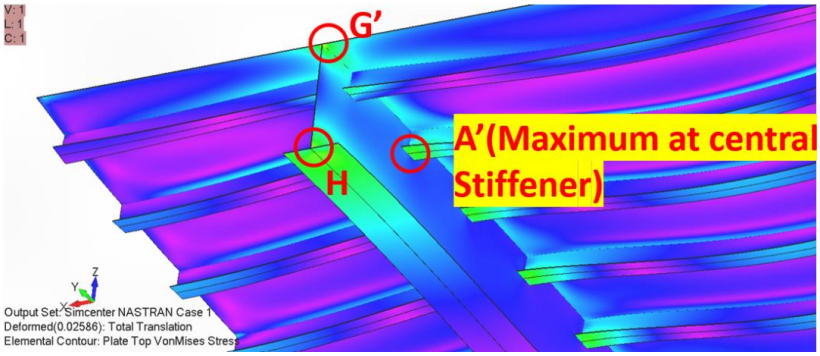

Figure 12. Points in the stiffened panel exposed to maximum von-mises stresses.

4. Theoretical calculation of the Normal Stresses

The obtained normal stress results from the FEA can also be manually determined by employing established theoretical principles and research findings. In this study, the normal stress distribution at the stiffener and plate is calculated. This process entails evaluating the stress distribution within an individual structure unit, as depicted in figure 13. This unit comprises the top plate and the stiffener. This structural arrangement is replicated to form the entirety of the stiffened deck. A notable contribution by Platypodis and Anyfantis [3] in their research has put forth the concept that the internal stress within stiffeners is a composite of stress arising from beam bending ($\sigma 1$) and stress

resulting from plate bending (σ2). Consequently, calculating the comprehensive internal stress within these structural elements necessitates a two-fold analysis. The process entails first computing the normal stress stemming from beam bending and subsequently evaluating the normal stress attributable to plate bending. In order to theoretically compute these stresses, it becomes necessary to make assumptions regarding the type of support (fixed, pinned, free) rendered by the stiffener and the plate within the stiffener panel. Despite the potentially intricate and nuanced real-world support conditions offered by the stiffener and girder, it is essential to approximate these conditions as one of the three mentioned support scenarios. It's worth acknowledging that such approximations can occasionally yield results that diverge significantly from actual conditions. However, theoretical calculations inherently possess limitations, and the approximation of support conditions becomes imperative.

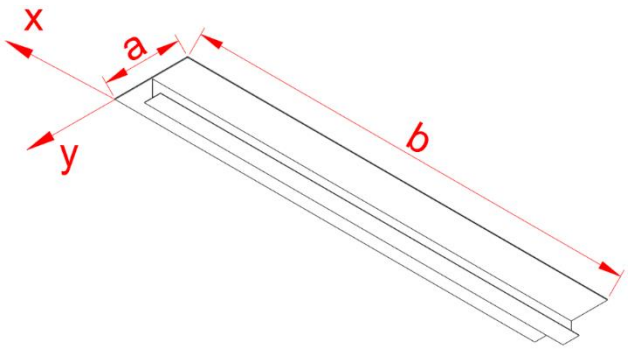

Figure 13. Schematic view of a single stiffener unit.

In this research, the assumption is made that both the girder and the stiffener offer fixed support. Although it's evident that this assumption is not entirely precise, as inform by the deflected shape observed in the outcome of FEA, both the stiffeners and girders exhibit deflection under stress. Nevertheless, considering that to some extent, translational and rotational movement is restricted at the connections with the stiffeners and girders, this assumption is deemed the most reasonable approach. As a consequence, the stiffener is assumed to be fixed at its ends where it interfaces with the girders. Additionally, each individual plate unit, possessing two edges connected to the girders and two edges connected to the stiffeners, is regarded as being clamped along all of its edges.

4.1. Beam bending stress calculation

To calculate the maximum stress caused by beam bending, the stiffener is conceptualized as a fixed-ended beam. The line load, q (N/m), is uniform along the beam and can be derived from the pressure, p (N/m2), on the plate. Classical beam theory proposes a specific bending moment distribution for this scenario as shown in figure 14, signifying that the maximum bending moments occur at the ends of the stiffener. The bending moment can be calculated as shown in equation (1) and equation (2).

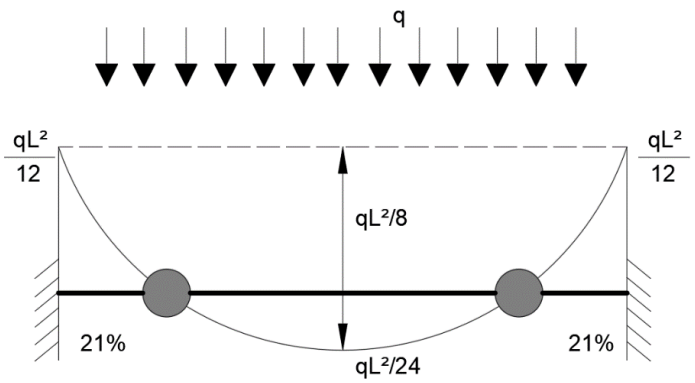

Figure 14. Bending moment diagram of a simple beam with two ends fixed.

$$q = p * b \tag{1}$$

$$M_{max} = \frac{qa^2}{12} \tag{2}$$

For determining the centroid of the cross-sectional area of the stiffener as shown in figure 15. the I-beam section is divided into three segments, as depicted in figure 16. The equation for finding the centroid of a multi-segment shape is utilized to determine the vertical centroid.

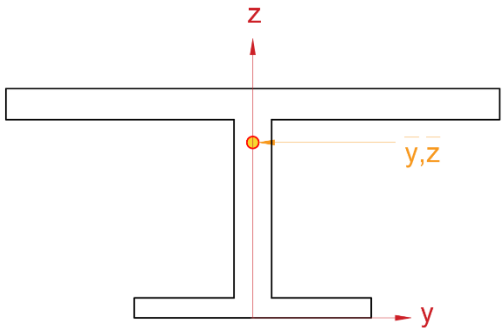

Figure 15. Axis and centroid of the cross section.

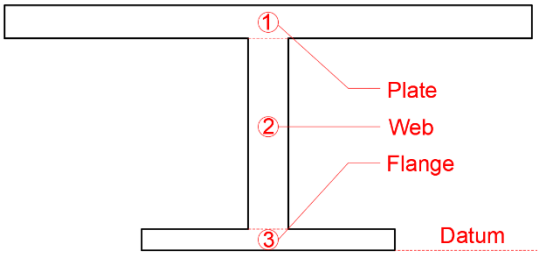

Figure 16. Individual segments of the cross section.

$$\bar{z} = \frac{\sum A_i z_i}{\sum A_i} \tag{3}$$

where A_i is the individual segment's area, z_i is the individual segment's centroid distance from the datum. Now, the Parallel Axis Theorem can be used to calculate the moment of inertia about the y axis.

$$I_y = \sum (I_{y,i} + A_i\, d_i^2) \tag{4}$$

where $I_{y,i}$ is the moment of inertia of the individual segment about its own centroid axis, d_i is the vertical distance from the centroid of the segment to the centroid of the entire cross-section.

With the moment of inertia I_y and the maximum bending moment M_{max} calculated, stress at any point along the z-axis can be determined. Following Euler-Bernoulli beam theory, the bending stress in the beam reaches its maximum at the farthest location from the neutral axis. Since tensile stress is present above the neutral axis, the maximum positive stress is expected to occur at the top of the beam, whereas the maximum negative stress is expected to occur at the bottom of the beam. Both the normal stresses at the top and bottom of the beam are calculated and compared to find the most extreme bending stress in the beam.

$$\sigma_{Top\ beam} = \frac{M_{max} * z_{top}}{I_y} = \frac{M_{max} * (h2 + h1 + Tp - \bar{z})}{I_y} \tag{5}$$

$$\sigma_{Bottom\ beam} = \frac{M_{max} * z_{bottom}}{I_y} = \frac{M_{max} * -\bar{z}}{I_y} \tag{6}$$

4.2. Plate bending stress

Numerous research studies have put forth methodologies for predicting stress distribution in a rectangular plate subjected to a clamped support condition at all four edges. Huges [11] highlighted that, in such cases, the maximum stresses are found at the midpoint of the plate's edge. Notably, the utmost stress magnitude occurs at the longer edge of the plate. Timoshenko [5], on the other hand, devised a table enabling the calculation of the maximum moment at the midpoint of these edges. This calculation is based on the plate width (b) and the uniform pressure (p). Given that the ratio of a/b exceeds 2 in this context, the corresponding formula can be expressed as presented in equation (7).

$$M_y = -0.0571 p b^2 \tag{7}$$

where M_y is the maximum moment at the mid-point of the plate's edge that span in the y direction.

After obtaining the bending moment through Timoshenko's table, the subsequent step involves calculating the bending stress using classical plate theory, as expressed in equation (8). Since the cross-section of the plate is a simple rectangular shape that it is symmetrical about its neutral axis. Therefore, the maximum and minimum normal stresses are situated at the top and bottom of the plate, respectively, and these stresses have equal magnitude. Moreover, stress variations occur linearly across the thickness of the plate.

$$M_y = -\int_{-\frac{tp}{2}}^{\frac{tp}{2}} z\sigma_{yy}dz = \frac{d\sigma_{yy}}{dz} * \frac{tp^3}{12} \tag{8}$$

$$\sigma_{Top\ plate} = \frac{d\sigma_{yy}}{dz} * \frac{tp}{2} \tag{9}$$

$$\sigma_{Bottom\ plate} = -\frac{d\sigma_{yy}}{dz} * \frac{tp}{2} \tag{10}$$

Alternatively, the bending stresses at the midpoints of the plate's edges can also be determined utilizing the graph formulated by Huges, visually depicted in figure 17. The coefficient value, denoted as k, can be extracted from the graph by considering the length-to-width ratio of the plate. Subsequently, the following equations are applied to determine the maximum stress at the designed point. Remarkably, it was observed that these two methodologies yield comparable outcomes.

$$\sigma_{Top\ plate} = kp\left(\frac{b}{Tp}\right)^2 \tag{11}$$

$$\sigma_{Bottom\ plate} = -kp\left(\frac{b}{Tp}\right)^2 \tag{12}$$

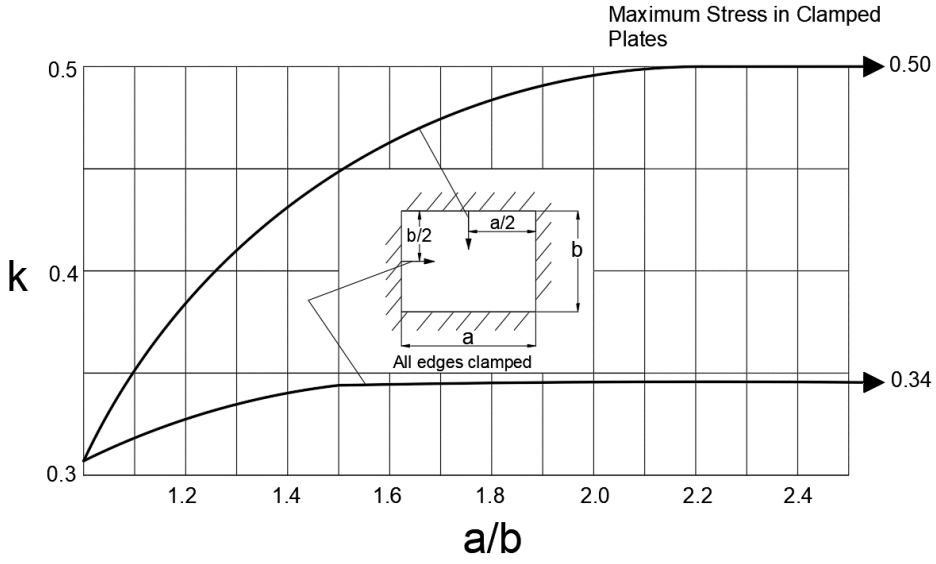

Figure 17. Plot to calculate maximum stress in rectangular plates with four edges clamped under uniform lateral pressure [5].

Having computed the stress contributions arising from both beam bending and plate bending, these values can be aggregated to derive the total stress across the cross-sectional area. The stress diagrams depicting the total internal stress within the stiffener are illustrated in figure 18.

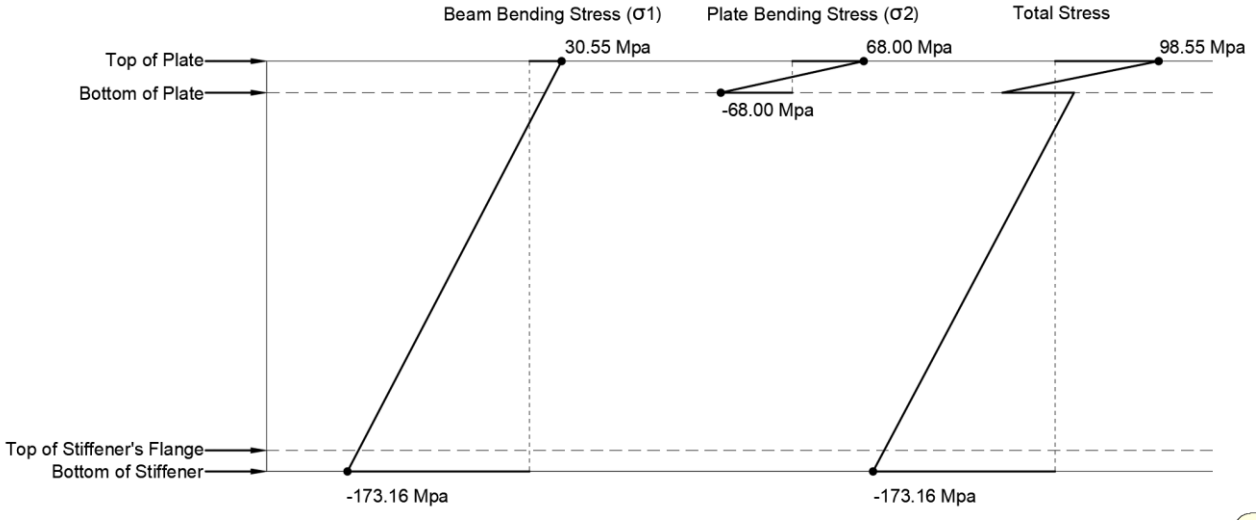

Figure 18. Illustration of the result of theoretical calculations

Table 4. Comparison of stress values computed from FEA and theoretical calculations.

Points	Location	Stress Type	Stress Direction	Stress Value from FEA (Mpa)	Stress Value from Theoretical Calculation (Mpa)	Difference (%)
A	The stiffener connected to the mid-span of the girders	Normal Stress	X	-184.79	-173.16	6.50
B				94.30	98.55	4.41
C				88.02	86.58	1.65

The results obtained from both the Finite Element analysis and theoretical calculations are presented in table 4. It is important to note that neither of these approaches can fully capture the precise actual stress within the structure under the given loading conditions. This discrepancy arises due to the inherent assumptions made in each respective method, leading to results that are approximations. Despite the limitations, the values derived from the two distinct approaches exhibit a remarkable degree of similarity. Furthermore, the percentage differences between the results obtained from them are consistently below 10%. This convergence strongly suggests the accuracy of the established finite element model and its successful alignment with the actual structure. As a result, the outcomes presented in this study are well-founded and justifiable.

5. Conclusion

In conclusion, stiffened panel structures play a crucial role in various domains such as ship deck applications. However, understanding their mechanical behavior and stress distribution remains a pivotal concern. This study aimed to simulate the stress behavior of stiffened panel structures under uniformly distributed loads, employing a combination of finite element analysis and theoretical calculations to elucidate the significant characteristics of internal normal stresses, shear stresses, and von Mises stresses within the structure. The accuracy and reliability of the analytical approach employed in this study were validated through a comparison between finite element modeling and theoretical analysis. The points in the structure that exhibit significant stress concentration have been presented. These quantitative stress data provide valuable insights for further refining the design and analysis methodologies of stiffened panel structures.

In the course of conducting FEA and theoretical calculations to assess the stress distribution within the stiffened panel, several assumptions have been made. These approximations were necessitated by the intricate support conditions of the structure and the overall complexity of the actual system. It is essential to acknowledge that these approximations can potentially result in disparities when compared to real-world conditions. Nevertheless, it is important to recognize that such

approximations are an inherent aspect of both theoretical calculations and FEA methodologies. The nature of the analysis demands simplifications to address the limitations of these methods. These approximations enable complex calculations for valuable insights into the structure's behavior.

In summary, this study provides in-depth insights into the stress behavior of stiffened panel structures, holding significance for enhancing the design and analysis approaches of such structures in the future. Exploring the impact of diverse loading conditions, advancing computational methods for more accurate modeling, conducting experimental validations, and optimizing design approaches are key areas of interest. By delving into these aspects, a deeper understanding of stiffened panel structures can be achieved, leading to improved designs, enhanced performance, and broader applicability in various industries.

Authors Contribution

All the authors contributed equally and their names were listed in alphabetical order.

References

[1] Zhang, Q., Yang, H., Wu, S., Cheng, W., Liang, Y., Huang, Y. (2023) A study on the ultimate strength and failure mode of stiffened panels. Journal of Marine Science and Engineering, 11: 1214-1234.

[2] Xu, M. C., Guedes Soares, C. (2013) Experimental study on the collapse strength of wide stiffened panels. Marine Structures, 30: 33-62.

[3] Platypodis, E. L., Anyfantis, K. N. (2022) On the modeling of ship stiffened panels subjected to uniform pressure loads. Applied Mechanics, 3: 125–143.

[4] Kim, D. K., Yu, S. Y., Lim, H. L., Cho, N.-K. (2020) Ultimate compressive strength of stiffened panel: An empirical formulation for flat-bar type. Journal of Marine Science and Engineering, 8: 605-628.

[5] Timoshenko, S., Woinowsky-Krieger, S. (1959) In Theory of Plates and Shells - 2nd Edition., McGraw-Hill, New York.

[6] Young, W. C., Roark, R. J. (2002) Roark's Formulas for Stress and Strain – 7th Edition, McGraw-Hill, New York.

[7] Wojtaszak, I. A. (1937) The calculation of maximum deflection, moment, and shear for uniformly loaded rectangular plate with clamped edges. Journal of Applied Mechanics, 4: 173-176.

[8] Aginam, C., Osadebe, N. (2011) Bending analysis of isotropic rectangular plate with all edges clamped: variational symbolic solution. Journal of Emerging in Engineering and Applied Sciences (JETEAS), 2: 846–852.

[9] Kelly, P. (2013) Solid Mechanics Part ii: Engineering Solid Mechanics Small Strain. https://pkel015.connect.amazon.auckland.ac.nz/SolidMechanicsBooks/Part_II/index.html.

[10] Fricke, W., Bronsart, R., Paik, J. K. (2012) Committee III.1 ultimate strength. In: Fricke, W., Bronsart, (Eds.), Proceedings of the 18th International Ship and Offshore Structures Congress (ISSC). Schiffbautechnische Gesellschaft e.V., Rostock. pp. 285-293.

[11] Hughes, O. F., Paik, J. K., Béghin, D. (2010) Ship structural analysis and design. Society of Naval Architects and Marine Engineers, New Jersey.